SOI Refractive Index Sensor Based on Tilted Bragg Gratings Mode Conversion

Eman A. Elzahaby[1,2], Ahmed M. R. Fath Elbab[1], and Hossam Shalaby[1,2], *Senior Member*, *IEEE*
[1]*Egypt-Japan University of Science and Technology (E-JUST), Alexandria 21934, Egypt*
[2]*Faculty of Engineering, Alexandria University, Alexandria 21544, Egypt*
eman@alexu.edu.eg, ahmed.rashad@ejust.edu.eg, shalaby@ieee.org

ABSTRACT
An integrated optical mode converter, based on tilted Bragg surface gratings in silicon-on-insulator technology, is designed to achieve features needed to promote a refractive index integrated sensor. The tilted grating is optimized to minimize device footprint (60 μm), and to obtain a narrow resonance full width at half maximum FWHM (7.3 nm) and a significant transmission dip (-10 dB). The proposed device achieves a linear response over a relative wide wavelength range, and a high sensitivity of 160 nm/RIU.
Keywords: Bragg gratings, integrated optics, optical sensors, silicon photonics, silicon-on-insulator.

1. INTRODUCTION

Recently, silicon-on-insulator platform has been widely used to implement label-free refractive index (RI) based sensors, for various applications of biomedical and chemical sensing [1]. Basically, sensing technique using waveguides relies on evanescent field of a propagating mode. The larger the field tail outside the waveguide is, the higher is the sensitivity that can be achieved. Typically, RI sensors based on non-tilted Bragg gratings were preferably designed with corrugations in sidewalls, rather than being on the surface, as the latter's performance has been reported to suffer from a lack in sensitivity, and long footprint [2].

In this paper, we introduce a simple RI sensor based on a mode converter, which is designed appropriately to couple optical power from the fundamental mode (TM_0) to a higher order mode (TM_2). The benefit of using a higher order mode is that it would have a higher field tail extending through sensing region, which increases sensitivity. Furthermore, we use TM modes because their confinement inside silicon is less than TE modes, which also contributes to sensitivity increase.

The proposed device uses a single strip waveguide assisted with surface tilted gratings, in which the gratings are tilted by an angle θ with respect to the direction of propagation [3]. The existence of this tilt angle gives a degree of freedom to couple between fundamental mode and any other higher order mode, with a relatively small number of Bragg gratings. This tilt angle allows us to implement a RI sensor with a higher sensitivity and shorter length compared to non-tilted structure investigated in [2].

The sensing functionality is achieved by measuring the change in the surrounding refractive index n_s through monitoring the shift in the resonance (Bragg) wavelength, at which mode coupling occurs.

We start by employing coupled-mode theory (CMT) to provide a comprehensive analysis of the proposed device [4], in order to find suitable values of grating parameters, including grating depth, duty cycle, and the required number of gratings. Then, we examine sensing characteristics of the proposed device, via MATLAB, when used as a liquid RI sensor.

2. MODELLING AND CHARACTERIZATION

Our model is based on considering a multimode strip silicon waveguide, with refractive index n_{si}, on top of SiO_2 BOX layer, and surrounded by a liquid with refractive index n_s, as an unperturbed region, where the perturbation is implemented by periodically etching tilted grooves, as shown in Fig. 1.

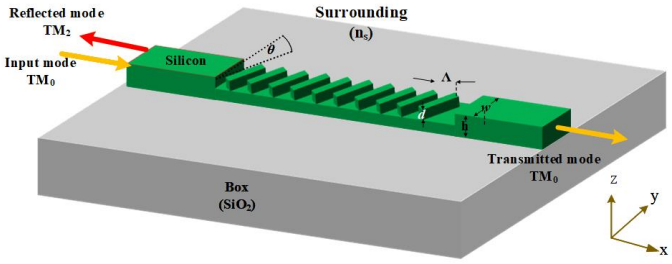

Figure 1. Schematic structure of tilted Bragg grating engrooved into strip silicon waveguide.

The refractive index distribution of the tilted Bragg grating inside the perturbed region is written as [3, 4]

$$\Delta n^2(y,z) = \sum_{m=-\infty}^{\infty} b_m \quad e^{jm2\pi y \tan(\theta)/\Lambda}, \tag{1}$$

where b_m and Λ represent, respectively, Fourier series coefficients of the periodic perturbation and the longitudinal grating period, along the x-axis, while θ is the tilt angle of the grating grooves with respect to the y-axis.

In our proposed device, gratings are designed appropriately so that coupling takes place between modes that propagate in contra directions. Accordingly, the normalized coupling coefficients can be calculated from

$$\kappa_{\nu,\mu}^{m} = \frac{\int_{-w/2}^{w/2}\int_{0}^{h} \psi_\nu(y,z)\Delta n^2 \psi_\mu^{*}(y,z)dydz}{\left[\left(\int_{-\infty}^{\infty}\int_{-\infty}^{\infty} \psi_\nu(y,z)\psi_\nu^{*}(y,z)dydz\right)\left(\int_{-\infty}^{\infty}\int_{-\infty}^{\infty} \psi_\mu(y,z)\psi_\mu^{*}(y,z)dydz\right)\right]^{1/2}}, \tag{2}$$

$$\delta = \beta_\nu + \beta_\mu - \frac{2\pi}{\Lambda}, \tag{3}$$

where $\kappa_{\nu,\mu}^{m}$ is the coupling coefficient between the fundamental TM_ν and the TM_μ modes due to the m^{th} grating order, ψ_ν and ψ_μ are the field profiles the unperturbed modes of order ν and μ, respectively, w is the waveguide width, h is the waveguide height, δ is phase mismatch factor, β_ν and β_μ are the propagation constants of the two modes.

Both the phase matching condition, which is obtained by setting Eq. (3) to zero, and coupling coefficients have essential roles. Indeed, the former is responsible for finding the required Bragg grating period, depending on the effective refractive indices of modes, and the latter is an indication of the coupling strength. The impact of the coupling coefficients is optimized in the next section.

3. RESULTS AND DISCUSSIONS

Through this section, we are going to show the impact of grating parameters, including tilt angle, duty cycle, and grating depth, on coupling coefficients. Next, the design of the proposed device is optimized to operate as a refractive index sensor. The performance of this sensor is examined numerically via MATLAB.

3.1 Coupling Coefficients Analysis

Using Eq. (2), coupling coefficients can be obtained by knowing the effective indices and magnetic fields of TM modes, using the effective index method EIM for a multimode waveguide of height $h = 220$ nm and width $w = 1.5$ µm, and refractive indices of $n_{Si} = 3.477$, $n_{SiO_2} = 1.44$, and $n_S = 1.33$.

We start by determining the grating period to be 400 nm, at which the phase matching condition is satisfied between the fundamental TM_0 and TM_2 modes. As shown in Fig. 2(a), we calculate coupling coefficients for a wide range of tilt angles, assuming fully etched grating with duty cycle of a half grating period (200 nm).

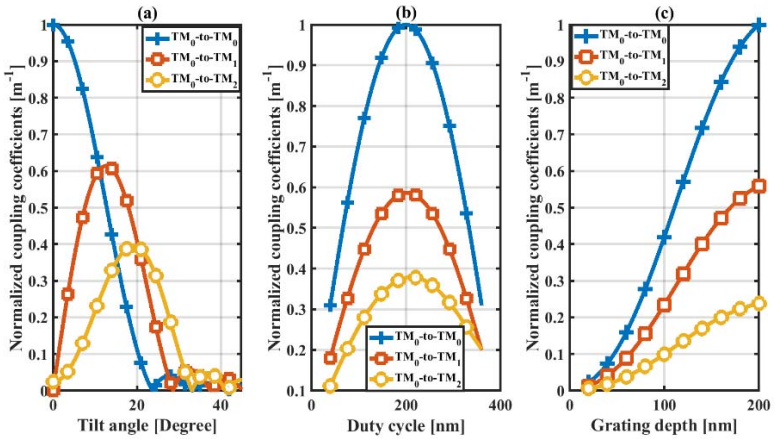

Figure 2. Variation of coupling coefficients versus: (a) tilt angle; (b) duty cycle; (c) grating depth.

One of the most important findings in this paper is that, for each mode, there is an optimum grating tilt angle, at which the coupling coefficient is maximum. Furthermore, the optimum tilt angle increases as the mode order increases, which means that the ability to design a mode converter from the fundamental mode to a higher order mode becomes more applicable. It is easily noticed that the optimum tilt angle is around 19°, in case of TM_0 to TM_2 coupling, on which we focus in this work.

In terms of duty cycle, the coupling coefficients are depicted in Fig. 2(b) at the optimum tilt angle of each mode, as obtained from Fig. 2(a), assuming a fully etched grating. It is evident that the maximum coupling coefficient, for the fundamental mode contra-coupling, takes place when duty cycle equals half of the period,

which has been verified in previous studies [4]. However, this is not the case for higher order modes, as the optimum duty cycle occurs at slightly greater than half a grating period. For TM_0-to-TM_1 and TM_0-to-TM_2 couplings, we calculate the duty cycles to be 202 and 210 nm, respectively.

By examining the impact of grating depth on coupling coefficients at the optimum values of both tilt angle and duty cycle, for each mode, one can notice, from Fig. 2(c), that all modes follow the same trend, coupling coefficients increase as the depth of the grating become dipper, as the refractive index perturbation becomes stronger, but the slope of growing raises as the mode order increases.

From the previous discussion, the augmentation in coupling strength is achieved by selecting the optimum tilt angle, duty cycle, and by subsiding grating depth. Meanwhile, these terms, except for grating tilt angle, have a significant effect on the overall performance of the proposed device, as will be illustrated below.

3.2 Investigating Device Parameters

Now, we will focus on designing a mode converter to couple power from TM_0 to TM_2 modes, and exploit the newly generated mode (TM_2) to sense variations of the surrounding region. We choose the TM_2 mode, as it possesses a relatively higher evanescent field in the sensing medium.

In Fig. 3(a), we plot the maximum reflectivity of the proposed device versus duty cycle, at a fixed number of gratings ($N = 80$), and assuming fully etched grating. In addition, the required number of gratings, to keep the maximum reflectivity constant at its optimum value (~0.98) over the entire range of duty cycle, is depicted. It is obvious that we are dealing with a trade-off. By increasing duty cycle, a turning point appears at which the maximum reflectivity has a peak of 0.98, and subsequently the corresponding number of gratings shows a minimum on the curve, which in turn leads to the least device length. Away from this turning point, the number of gratings needs to be increased to restore maximum reflectivity at 0.98. It is worth noticing that the above findings come in accordance with coupling coefficients profile, shown in Fig. 2(b).

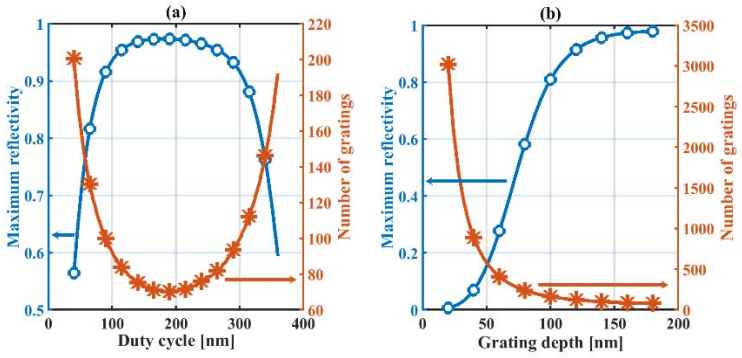

Figure 3. Variation of maximum reflectivity and number of gratings versus: (a) duty cycle; (b) grating depth.

Next, in the same manner, we examine the behaviour of the previously mentioned parameters versus grating depth, at a fixed duty cycle of 210 nm, in Fig. 3(b). It reveals that the impact of increasing grating depth is translated to increasing the maximum reflectivity while decreasing the required number of gratings at which the maximum reflectivity equals 0.98, because of the associative increase in coupling coefficient, as shown in Fig. 2(c).

In addition, as we seek to design a refractive index sensor, it is important to make its response selective as much as possible by narrowing the full width at half maximum power (FWHM). Figures 4(a) and 4(b) respectively show the variations of FWHM versus both of duty cycle, while grating depth is kept fixed at 220 nm, and grating depth, at a fixed duty cycle of 210 nm, considering the number of gratings to be 80. It is noticed that, when increasing duty cycle, the FWHM rises until a turning point comes into view, at which it begins to decline. On the other hand, the diminution of grating depth causes a reduction in FWHM. One can notice that the above observed attitude of FWHM resembles that of maximum reflectivity, shown in Figs. 3(a) and 3(b) (blue curves). Indeed, this behaviour is originally attributed to coupling coefficient profile, which is declared in Figs. 2(b) and 2(c).

As a compromise between the attained reflectivity and the FWHM, on the one hand, and the associative number of gratings, on the other hand, we choose to design grating with a duty cycle and grating depth of 50 and 150 nm, respectively. The corresponding values of maximum reflectivity, FWHM, and number of gratings are 0.98, 7.3 nm and 150, respectively. At this stage, we examine the performance of our design of the RI sensor by observing the shift in resonance wavelength as surrounding RI changes, in Fig. 5(a). As our sensor is designed to exploit a higher order mode (TM_2), it is worth noticing the high sensitivity, which is calculated as 160 nm/RIU.

Finally, it should be remarked that the available grating couplers usually transfer light from chip to fiber, and vice versa, through the fundamental mode, whereas our sensor is based on reflecting a higher order mode. Fortunately, we can detect the shift in wavelength by observing the transmission, instead of the reflection. That

is because the maximum reflectivity of the TM_2 mode at Bragg wavelength corresponds to a minimum on the transmission profile of the fundamental TM_0 mode. Accordingly, we can search for a transmission dip on the analyzer, as shown in Fig. 5(b), instead of searching for a peak point of reflection.

It is worth highlighting that our proposed RI sensor introduces a significant reduction in device length, by about 65%, compared with that reported in [2], while the sensitivity is improved from 33 nm/RIU to 160 nm/RIU.

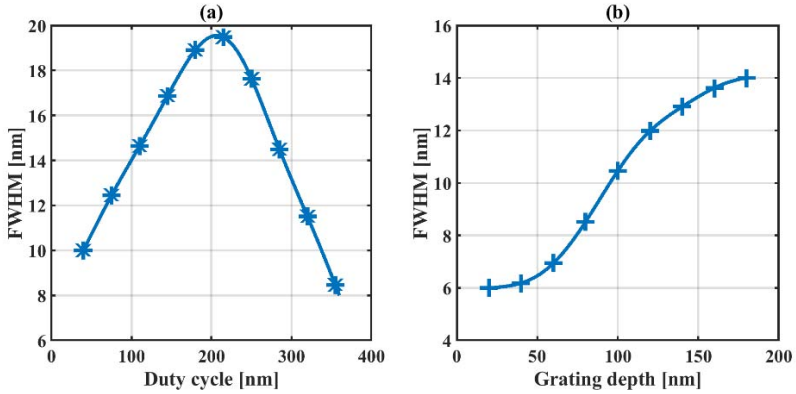

Figure 4. Variation of the FWHM versus: (a) duty cycle; (b) grating depth.

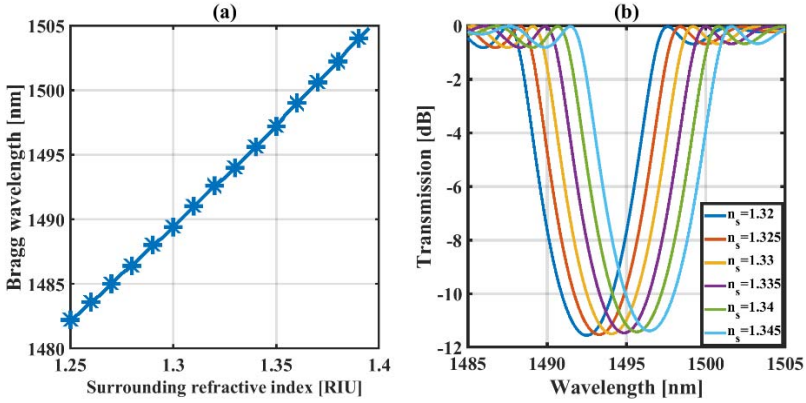

Figure 5: (a) Variation of the Bragg resonance with surrounding refractive index; (b) Spectral response of tilted Bragg grating for different surrounding refractive indices.

4. CONCLUSIONS

In this paper, a label-free RI sensor based on a single waveguide mode converter utilizing reflective tilted Bragg gratings is designed to obtain the parameters needed for reliable sensing performance. The tilted gratings are investigated to find its optimum dimensions required to decrease sensor length (60 μm), and to obtain narrow FWHM (7.3 nm) with high sensitivity (160 nm/RIU), which are promising results, noticing that we use SOI platform only without adding extra layers from other material. The proposed sensor in this work is relatively compact, compared with other surface Bragg grating sensors, with reduction in length is about 65%, whereas the sensitivity is enhanced by about fivefold.

ACKNOWLEDGEMENTS

This work is financially supported by the Ministry of Higher Education, Egypt (MoHE).

REFERENCES

[1] E. Luan *et al.*: Silicon photonic biosensors using label-free detection, *Sensors*, vol. 18, no. 10, pp. 3519-3561, 2018.

[2] V. M. N. Passaro *et al.*: Design of Bragg grating sensors based on submicrometer optical rib waveguides in SOI, *IEEE Sensors Journal*, vol. 8, no. 9, pp. 1603-1611, Sep. 2008.

[3] H. Ma *et al.*: Tilted waveguide gratings and implications for optical waveguide-ring resonator, *J. of Lightwave Tech.*, vol. 33, no. 19, pp. 4176-4183, Oct. 2015.

[4] A. Yariv and M. Nakamura: Periodic structures for integrated optics, *IEEE Journal of Quantum Electronics*, vol. 13, no. 4, pp. 233-253, 1977.